Progress In Electromagnetics Research, PIER 65, 59–69, 2006

NUMERICAL ANALYSIS OF A SMALL ULTRA WIDEBAND MICROSTRIP-FED TAP MONOPOLE ANTENNA

A. A. Eldek

Department of Computer Engineering
Jackson State University
JSU Box 17098, Jackson, MS 39217-0198, USA

Abstract—This paper presents a planar microstrip-fed tab monopole antenna for ultra wideband wireless communications applications. The impedance bandwidth of the antenna is improved by adding slit in one side of the monopole, introducing a tapered transition between the monopole and the feed line, and adding two-step staircase notch in the ground plane. Numerical analysis for the antenna dimensional parameters using Ansoft HFSS is performed and presented. The proposed antenna has a small size of 16 × 19 mm, and provides an ultra wide bandwidth from 2.8 to 28 GHz with low VSWR level and good radiation characteristics to satisfy the requirements of the current and future wireless communications systems.

1. INTRODUCTION

From mobile telephones to wireless Internet access to networked appliances and peripherals, there is an increasing reliance on wireless communications to provide functionality for products and services. Therefore, the technologies for wireless communications always need further improvement to satisfy higher resolution and data requirements. That is why ultra wideband (UWB) communications systems covering 3.1 GHz to 10.6 GHz released by the Federal Communications Commission (FCC) in 2002 [1] are currently under development. However, there is always an increasing demand for smaller size, and greater capacities and transmission speeds, which will certainly require more operating bandwidth in the near future.

In the last few years, researchers have investigated several kinds of microstrip slot and printed antennas for UWB applications [2–15]. One of the best antennas in the last decade is the tap monopole antenna. The planar tap monopole antennas have been adopted and studied extensively for UWB communications systems because of their many appealing features. These features include wide impedance bandwidth, simple structure, small size, low profile, and omni-directional radiation patterns. Number of wideband tap monopole configurations, such as rectangular, elliptical, pentagonal, and hexagonal has been proposed for UWB applications [5:15]. Wide impedance bandwidth of (1:1.7), (1:2.25), (1:2.87), (1:3.4), (1:3.5), (1:3.7), (1:3.75) and (1:10.7) for VSWR<2, and an antenna size of 20, 24, 20, 23, 16, 26, 30, and more than 52 mm are reported in [7–14], respectively.

Recently, we presented a modified printed tap monopole antenna for UWB applications with a slit, notched ground plane, and tapered transition between the tap monopole and the feed line with a very wide impedance bandwidth of (1:7.9) [15]. In this paper, we present numerical analysis of the antenna in [15] to show the effect of each dimensional parameter. The numerical analysis results in a much better bandwidth of (1:10), with a low VSWR level of less than 1.75, and a small size of 16 mm, which is smaller than the antennas presented in [2–14]. The results in this paper are obtained from Ansoft HFSS simulations, which are based on the Finite Element Method (FEM). Verification of the final results is performed using a FDTD based code designed by the author.

2. ANTENNA GEOMETRY AND PARAMETERS

The geometry and parameters of the proposed broadband tap monopole antenna are depicted in Fig. 1. The antenna is printed on an FR4 Epoxy substrate with a relative dielectric constant (ε_r) of 4.4, a tangential loss ($\tan\sigma$) of 0.02, a thickness (h) of 1.6 mm, a width (W_s) of 16 mm and a length (L_s) of 19 mm. The basic antenna structure consists of a rectangular patch with a narrow slit, a tapered transition, a feedline, and a truncated ground plane with a two-step staircase notch.

The rectangular patch has a width P_1 and a height P_2. A narrow slit of width S_1 and depth S_2 is cut on the patch's right side and placed at a distance S_3 away from the lower right corner of the patch. The slit is placed to create additional path for the surface current, which produces an additional resonance, and as a result, increases the bandwidth when the dimensions are properly chosen, which is proven in [15] by comparing VSWRs for antennas with and without slit. Additionally, because this slot is very narrow it does not disturb the existing resonances of the tap monopole.

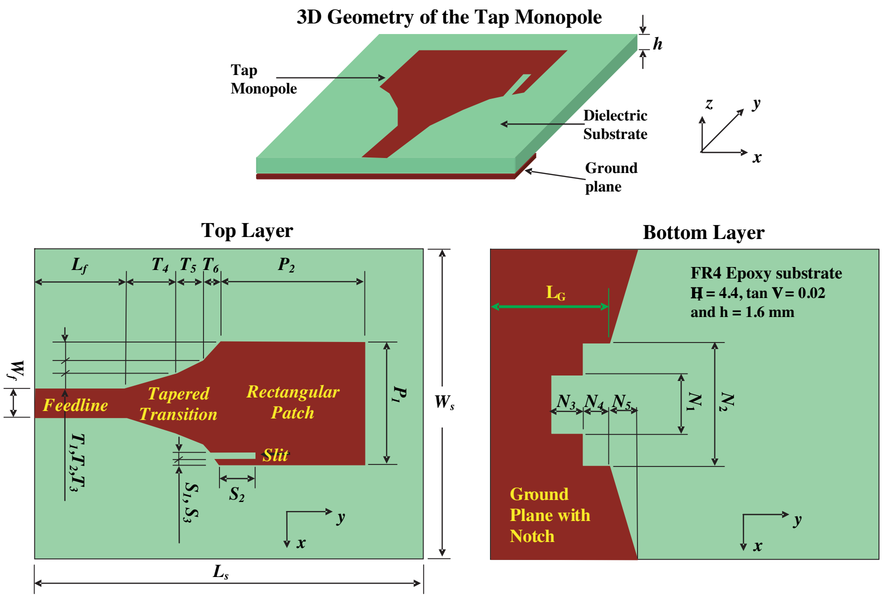

Figure 1. The geometry and parameters of proposed planar tap monopole antenna.

The patch is connected to a feed line of width W_f and length L_f through a tapered transition, which is defined by the parameters T_1 to T_6, as shown in Fig. 1. The tapering produces a smooth transition, which reduces the reflections resulting from the sudden change from the feedline width to the patch width.

On the other side of the substrate, a conducting ground plane of width $= W_s$ and length $= L_G$ is placed. The truncated ground plane is playing an important role in the broadband characteristics of this antenna, because it helps matching the patch with the feedline in a wide range of frequencies. This is because the truncation creates a capacitive load that neutralizes the inductive nature of the patch to produce nearly-pure resistive input impedance.

To further enhance the matching, a two-step staircase notch is embedded in the truncated ground plane. The notch is defined by the parameters N_1 to N_4 as depicted in Fig. 1. In addition, two triangles of height $= N_5$ are added at the notch sides. The two-step staircase notch and the two triangles are used to control the impedance bandwidth and return loss level by modifying the capacitance between the patch and the ground plane.

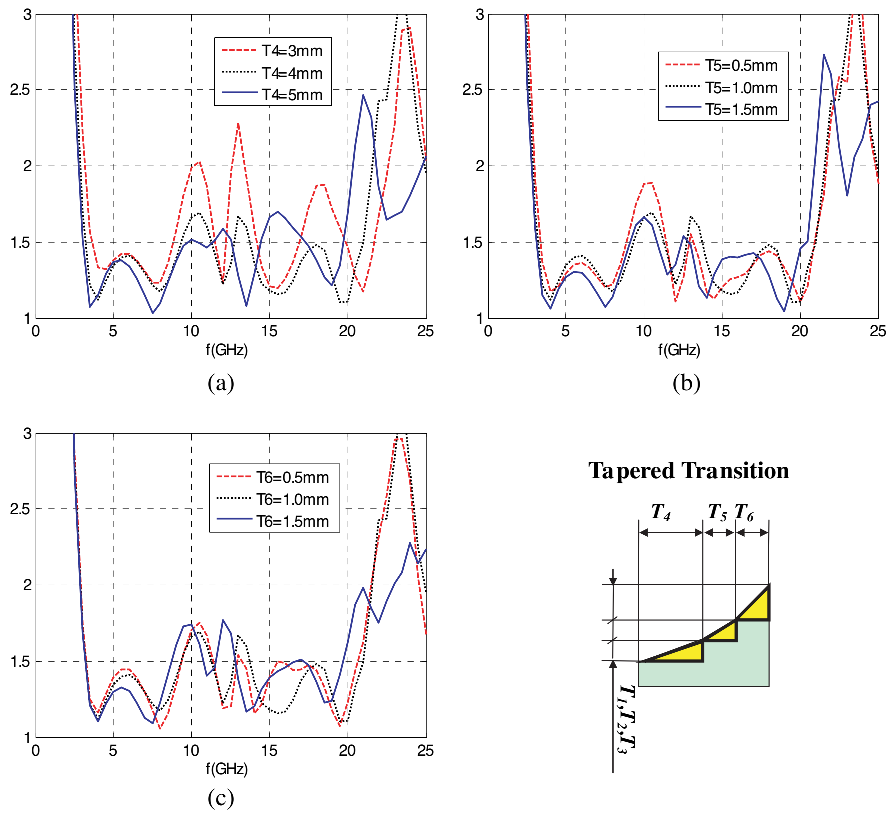

Figure 2. The effect of the tapered transition parameters (a) T_4, (b) T_5, and (c) T_6.

3. NUMERICAL ANALYSIS

The parameters of this antenna are studied by changing one parameter at a time and fixing the others. The initial dimensions of the antenna are as follows: (1) Substrate: $W_s = 16$, $L_s = 19$, (2) Patch and Slit: $P_1 = 7$, $P_2 = 9$, $S_1 = 0.3$, $S_2 = 2.5$, $S_3 = 0.5$, (3) Tapered Transition: $T_1 = 1$, $T_2 = 0.75$, $T_3 = 0.75$, $T_4 = 4$, $T_5 = 1$, $T_6 = 1$, (4) Feedline: $W_f = 2$, $L_f = 3$, and (5) Ground and Notch: $L_G = 4$, $N_1 = 7$, $N_2 = 5$, $N_3 = 1.5$, $N_4 = 1$, $N_5 = 0\,\text{mm}$.

In this study, the parameters T_4:T_6, S_1:S_3 and N_1:N_5 are presented in Figs. 2, 3 and 4, respectively, to show the effect of the tapered transition, the slit, and the notch on the VSWR of the antenna. The VSWR is computed over a large bandwidth from 2 to 25 GHz using

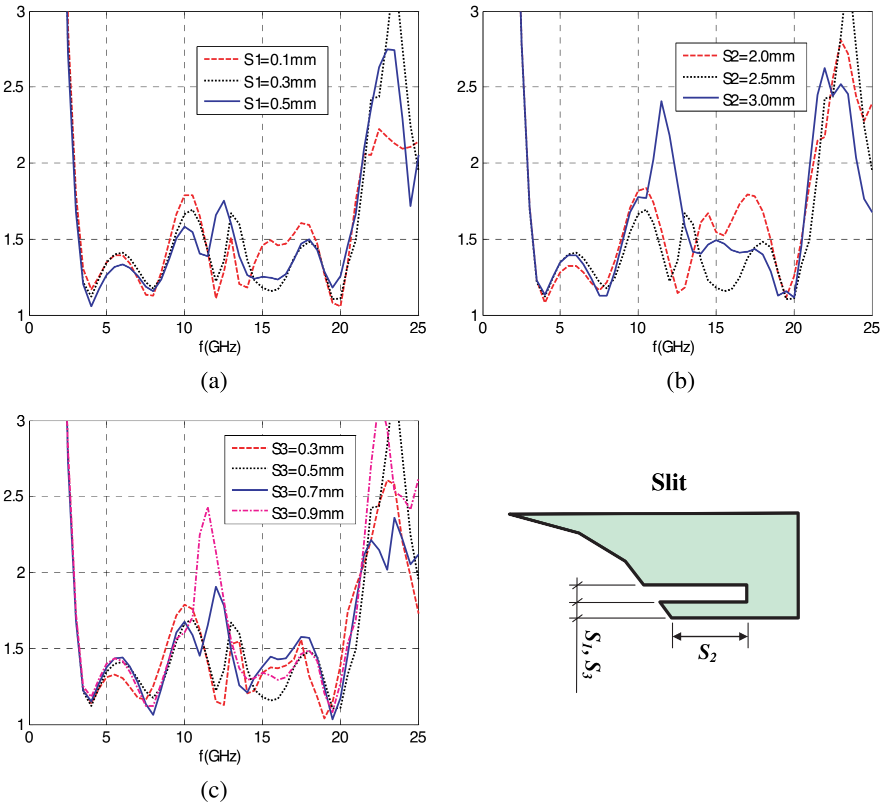

Figure 3. The effect of the slit parameters (a) S_1, (b) S_2, and (c) S_3.

the commercial computer software package HFSS of Ansoft.

Figure 2 shows the effects of T_4, T_5 and T_6. Generally, increasing these parameters improves the overall VSWR level because the transition from the feedline to the monopole becomes smoother. The parameter T_4 has more effect in the middle range. In addition, increasing T_4 decreases the upper operating frequency resulting in decreasing the bandwidth after $T_4 = 5\,\text{mm}$. The parameter T6 can be used to improve the VSWR at higher frequency, resulting in improving the bandwidth. The maximum bandwidth occurs at $T_6 = 1.5\,\text{mm}$.

On the other hand, the effects of the slit parameters are shown in Fig. 3. Increasing the slit width S_1 does not have significant effect. This may be because of the low coupling between the currents on the sides of the slit. The slit length S_2 and the slit distance from the edge S_3 control the VSWR level at 11.5 GHz. This is mainly because these

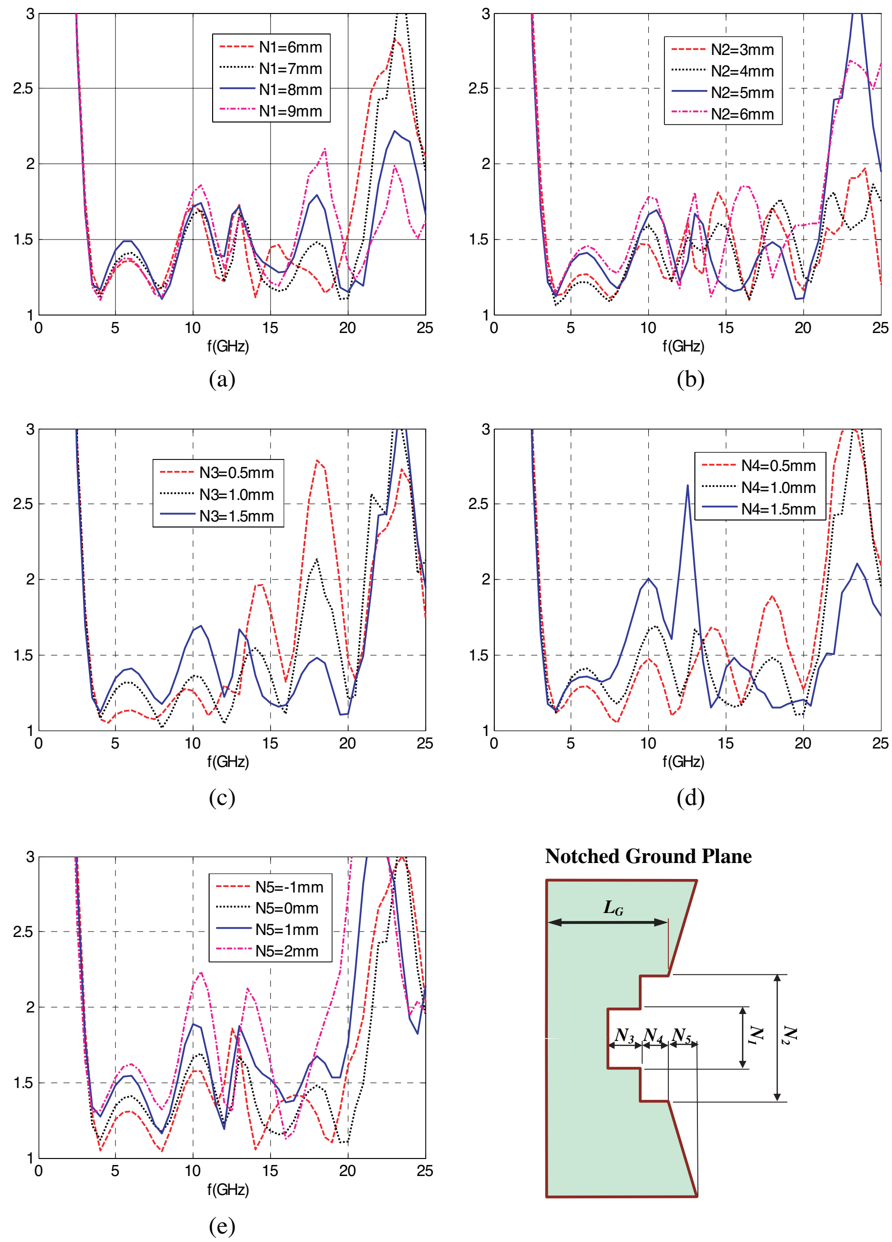

Figure 4. The effect of the notch parameters (a) N_1, (b) N_2, (c) N_3, (d) N_4, and (e) N_5.

two parameters control the impedance of the arm to the right of the slit, which can be considered an open circuit stub.

Figure 4 shows the effect of the notch parameters in the ground plane, which mainly affect the capacitance between the monopole and the ground plane. The overall capacitance is equivalent to number of capacitors connected together in parallel. N_1 and N_2 control the number of capacitors while N_3 and N_4 control their different capacitances. N_5 is another parameter for smoothing the notch and matching the feedline with the monopole. N_1 and N_2 have a clear effect at higher frequencies because they control the total capacitance. When N1 increases and N_2 decreases the VSWR level decreases. The best bandwidth is obtained when $N_2 = 4\,\text{mm}$, where the antenna operates from 2.8 to more than 25 GHz. The parameters N_3 and N_4 affect the VSWR level at the entire band. Increasing N_3 and N_4 improve the VSWR at higher frequencies, and increase it at the middle range between 4 and 13 GHz. Finally, increasing N_5 is found not to be helpful because it increases the VSWR level. The zero value of N_5 gives the best performance in terms of bandwidth and VSWR level.

4. FINAL DESIGN

The best bandwidth and VSWR level are obtained for the antenna with $N_2 = 4\,\text{mm}$, where the antenna is still working after 25 GHz. Therefore the VSWR is recomputed up to 30 GHz using Ansoft HFSS. Furthermore, to verify the results of HFSS, the antenna is simulated using our own FDTD code with CPML boundary [16]. In FDTD, the spatial increments $(\Delta x, \Delta y, \Delta z) = (0.05, 0.05, 0.2\,\text{mm})$, and a Gaussian waveform was used for excitation. A total number of 10000 time steps were used in order to ensure that the time domain response approaches zero.

A comparison between the computed VSWR and input impedance real and imaginary parts using HFSS and FDTD is presented in Fig. 5. Good agreement is observed which validates the design procedure using HFSS. The little differences between the two results are because of using stair case in FDTD to model the transition part, which affects the results, especially at higher frequencies, where $\Delta x/\lambda$ is relatively high.

Both results show that the antenna operates over a wide range that extends from 2.8 to 28 GHz, which is (1:10). The VSWR level is less than 1.75 in almost the entire operating band. The low VSWR level results from the tapered transition and the good matching achieved by the two-step staircase notch. The average value of the real part of the resulting input impedance is approximately 50Ω, while the

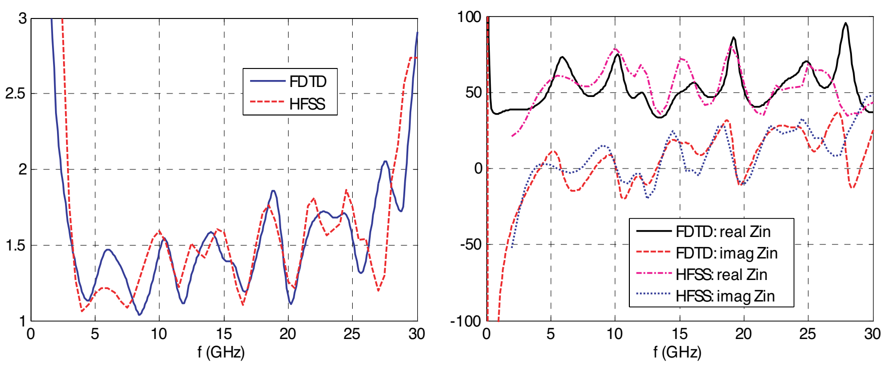

(a) (b)

Figure 5. Computed (a) VSWR and (b) Input impedance, using HFSS and FDTD for a tap monopole of $W_s = 16$, $L_s = 19$, $P_1 = 7$, $P_2 = 9$, $S_1 = 0.3$, $S_2 = 2.5$, $S_3 = 0.5$, $T_1 = 1$, $T_2 = 0.75$, $T_3 = 0.75$, $T_4 = 4$, $T_5 = 1$, $T_6 = 1$, $W_f = 2$, $L_f = 3$, $L_G = 4$, $N_1 = 7$, $N_2 = 4$, $N_3 = 1.5$, $N_4 = 1$, and $N_5 = 0$ mm.

imaginary part is slightly fluctuating around zero value. This proves the aforementioned explanation of the effect of truncating the ground plane, and introducing a stair case notch inside it, in producing almost pure resistive input impedance.

Although the change in the antenna dimensions results in a considerable enhancement in the antenna bandwidth from (1:7.9) to (1:10), this change does not significantly change the radiation patterns and the antenna gain. In fact, the far field characteristics of this antenna are quite similar to those of the antenna in [15], as depicted in Figs. 6 and 7, which show the radiation patterns for the final design at 5, 10, 15, 20, and 25 GHz. In the E-plane, as shown in Fig. 6, the antenna provides almost dipole-like radiation patterns in entire band that are deteriorated little at higher frequencies and affected by the truncated ground plane. In the H-plane, as depicted in Fig. 7, the antenna provides quasi omni-directional at 5 and 10 GHz, then starts to produce four major lobes at 15 GHz. The antenna provides an approximate average gain of 4 dB in the entire operating band.

The next step will be building and measuring this antenna, which is not possible at this moment because we do not have equipment at Jackson State University. However, the measurement may not be required to verify the HFSS and FDTD results, since they have been already verified by the good comparison between their results.

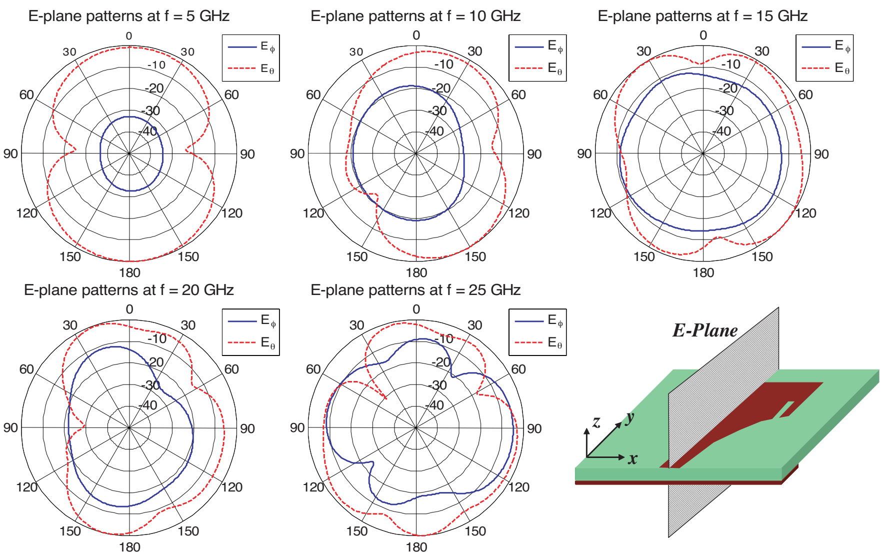

Figure 6. The computed co (E_θ) and cross (E_ϕ) polarized radiation patterns in the E-plane (y-z).

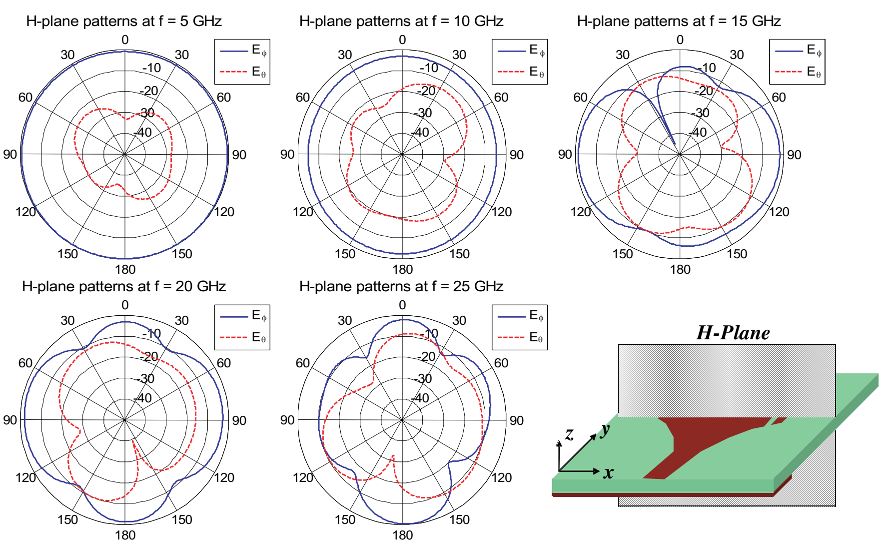

Figure 7. The computed co (E_θ) and cross (E_ϕ) polarized radiation patterns in the H-plane (x-z).

5. CONCLUSION

This paper presents a numerical analysis and design of a printed tap monopole antenna with a small size for UWB wireless communications applications. A slit, tapered transition and two-step staircase notch are implemented to obtain the ultra wide bandwidth of the antenna. The presented antenna exhibits an ultra wide impedance bandwidth of 1:10, with a low VSWR level of less than 1.75, and a small size compared to the UWB antennas reported recently. This antenna is a good candidate for hand-held UWB applications.

REFERENCES

1. FCC, "First report and order on ultra-wideband technology," Tech. Rep., 2002.
2. Eldek, A. A., A. Z. Elsherbeni, and C. E. Smith, "Rectangular slot antenna with patch stub for ultra wideband applications and phased array systems," *Progress In Electromagnetics Research*, PIER 53, 227–237, 2005.
3. Eldek, A. A., A. Z. Elsherbeni, and C. E. Smith, "Dual-wideband square slot antenna with a U-shaped printed tuning stub for wireless communication systems," *Progress In Electromagnetics Research*, PIER 53, 319–333, 2005.
4. Eldek, A. A., A. Z. Elsherbeni, and C. E. Smith, "Square slot antenna for dual wideband wireless communication systems," *J. of Electromagn. Waves and Appl.*, Vol. 19, No. 12, 1571–1581, 2005.
5. Chen, Z. N., M. W. Y. Chia, and M. J. Ammann, "Optimization and comparison of broadband monopole," *Proc. Inst. Elect. Eng.*, Vol. 150, No. 6, 429–435, Dec. 2003.
6. Antonino-Daviu, E., M. Cabedo-Fbre's, M. Ferrando-Bataller, and A. Valero-Nogueira, "Wideband double-fed planar monopole antennas," *Electronic Lett.*, Vol. 39, No. 23, 1635–1636, Nov. 2003.
7. Lin, C. C., Y. C. Kuo, and H. R. Chuang, "A planar triangular monopole antenna for UWB communication," *IEEE Microwave and Wireless Components Lett.*, Vol. 15, No. 10, 624–626, Oct. 2005.
8. Al Sharkawy, M., A. A. Eldek, A. Z. Elsherbeni, and C. E. Smith, "Design of wideband printed monopole antenna using WIPL-D," *The 20th Annual Review of Progress in Applied Computational Electromagnetics, ACES'04*, Syracuse, NY, Apr. 2004.
9. Klemm, M. and G. Troester, "EM energy absorption in the human

body tissues due to UWB antennas," *Progress In Electromagnetics Research*, PIER 62, 261–280, 2006.
10. Gao, Y., B. L. Ooi, and A. P. Popov, "Band-notched ultra-wideband ring-monopole antenna," *Microwave Opt. Tech. Lett.*, Vol. 48, No. 1, 125–126, Jan. 2006.
11. Junh, J., W. Choi, and J. Choi, "A small wideband microstrip-fed monopole antenna," *IEEE Microwave and Wireless Components Lett.*, Vol. 15, No. 10, 703–705, Oct. 2005.
12. Chung, K., J. Kim, and J. Choi, "Wideband microstrip-fed monopole antenna having frequency band-notch function," *IEEE Microwave and Wireless Components Lett.*, Vol. 15, No. 11, 766–768, Nov. 2005.
13. Choi, S. H., J. K. Park, S. K. Kim, and J. Y. Park, "A new ultra-wideband antenna for UWB applications," *Microwave Opt. Tech. Lett.*, Vol. 40, No. 5, 399–401, Mar. 2004.
14. Agrawall, N. P., G. Kumar, and K. P. Ray, "Wide-band planar monopole antennas," *IEEE Trans. Antennas Propag.*, Vol. 46, No. 2, 294–295, Feb. 1998.
15. Eldek, A. A., "A small ultra wideband planar tap monopole antenna with slit, tapered transition and notched ground plane," *Microwave Opt. Tech. Lett.*, Vol. 48, No. 8, 1650–1654, Aug. 2006.
16. Roden, J. A. and S. D. Gedney, "Convolutional PML (CPML): An efficient FDTD implementation of the CFS-PML for arbitrary media," *Microwave Opt. Tech. Lett.*, Vol. 27, No. 5, 334–339, Dec. 2000.